Ordering and spin waves in $NaNiO_2$: A stacked quantum ferromagnet

M. J. Lewis,[1] B. D. Gaulin,[1,2] L. Filion,[1] C. Kallin,[1,2] A. J. Berlinsky,[1,2] H. A. Dabkowska,[1] Y. Qiu,[3,4] and J. R. D. Copley[3]
[1]*Department of Physics and Astronomy, McMaster University, Hamilton, Ontario, L8S 4M1, Canada*
[2]*Canadian Institute for Advanced Research, 180 Dundas Street West, Toronto, Ontario, M5G 1Z8, Canada*
[3]*National Institute of Standards and Technology, 100 Bureau Drive, Gaithersburg, Maryland, 20899-8562, USA*
[4]*Department of Materials Science and Engineering, University of Maryland, College Park, Maryland, 20742, USA*
(Received 25 February 2005; revised manuscript received 21 April 2005; published 5 July 2005)

Neutron scattering measurements on powder $NaNiO_2$ reveal magnetic Bragg peaks and spin waves characteristic of strongly correlated $s=1/2$ magnetic moments arranged in ferromagnetic layers which are stacked antiferromagnetically. This structure lends itself to stacking sequence frustration in the presence of mixing between nickel and alkali metal sites, possibly providing a natural explanation for the enigmatic spin glass state of the isostructural compound, $LiNiO_2$.

DOI: 10.1103/PhysRevB.72.014408 PACS number(s): 75.25.+z, 75.40.Gb, 75.50.Ee, 83.85.Hf

I. INTRODUCTION

Low-dimensional quantum magnets are well appreciated as fertile ground for spin liquid and other exotic quantum states of matter.[1] $NaNiO_2$ and $LiNiO_2$ are isostructural nickel-based quantum magnets with layered triangular structures. The enigmatic magnetic phase behavior associated with $LiNiO_2$ has been the subject of speculation for two decades.[2–9] This speculation has been largely fueled by the absence of observed transitions to long-range magnetic and orbital order in $LiNiO_2$. In contrast $NaNiO_2$ is known to undergo a Jahn-Teller structural distortion at high temperatures signalling orbital order,[10] and a low temperature anomaly in its susceptibility is often associated with long-range antiferromagnetic order.[11] However, like $LiNiO_2$, no definitive magnetic neutron scattering signature of such an ordered state has been observed in $NaNiO_2$ until now. We report the observation of magnetic Bragg peaks and spin wave scattering in $NaNiO_2$, which establishes its relatively simple magnetic structure and which may shed light on why $LiNiO_2$ has difficulty finding an ordered state at low temperatures.

Both $NaNiO_2$ and $LiNiO_2$ are comprised of stackings of triangular layers which alternate between NiO and AO, where A is either Li^+ or Na^+, as shown schematically in Fig. 1. The distance between neighboring triangular layers of magnetic Ni along the c direction is about 5.2 Å. Most of the extensive preceding work associated with the magnetism in these materials, assumes a low spin Ni^{3+} $s=1/2$ magnetic moment. However, some discussion of nickel in the $s=1$ Ni^{2+} oxidation state bound to an 1/2 hole on a neighboring O^- ion, resulting in an $s=1/2$ Zhang-Rice singlet, has been offered.[12,13] In both scenarios, either the nickel spin itself or the composite NiO spin is an extreme $s=1/2$ quantum mechanical entity, and a saturation magnetization corresponding to 1 μ_B per formula unit is observed in both $NaNiO_2$ and $LiNiO_2$.[14]

The possibility of antiferromagnetic coupling between these quantum moments within the triangular plane has generated much interest in the materials. The potential for geometrical frustration and exotic quantum ground states under such conditions has been well appreciated since Anderson[15] suggested a collective singlet, resonating valence bond ground state without long-range order for such a system. Indeed this possibility figures prominantly in the discussion of both early and more recent experimental work on $LiNiO_2$.[2,7] More generally, it is well known that the combination of antiferromagnetism and certain lattice symmetries based on triangles and tetrahedra leads to phenomena known broadly as geometrical frustration.[16]

As mentioned above, the possibility of such exotic behavior has been motivated, in part, by the absence of direct experimental signatures of conventional magnetic ordering, such as the observation of magnetic Bragg peaks by neutron diffraction. Given the difficulties associated with the study of these materials, it is a small wonder that progress has been slow. To date they have been available only as polycrystalline materials and, with a single $s=1/2$ magnetic moment per formula unit, the moment density is low. In addition, $LiNiO_2$ contains Li, whose strong neutron absorbtion is problematic for neutron scattering measurements. Finally, it is known that the similarity in ionic radii between Li^+ and Ni^{3+}, both ~0.7 Å, leads to mixing between these two sublattices,[3] further complicating the magnetic behavior of $LiNiO_2$. With an ionic radius of ~1 Å, Na^+ is a much larger ion, which makes such mixing unlikely. For these latter two reasons, one expects $NaNiO_2$ to be more amenable to a neutron scattering study than $LiNiO_2$.

II. MATERIALS AND EXPERIMENTAL METHODS

$NaNiO_2$ crystallizes into the rhombohedral space group $R3m$ at high temperatures, before undergoing a cooperative Jahn-Teller distortion leading to a structure with the space group $C2/m$ below ~480 K.[10,17] This structural phase transition lifts the orbital degeneracy between the $|3z^2\text{-}r^2\rangle$ and $|x^2\text{-}y^2\rangle$ states within the e_g doublet in $NaNiO_2$.[10] The resulting room temperature structure[10] in $NaNiO_2$ is characterized by lattice parameters $a=5.31$ Å, $b=2.84$ Å, $c=5.57$ Å, and $\beta=110.44°$, and the structure no longer displays edge-shared, equilatoral triangles within the a-b plane.

A similar structural distortion does not obviously occur in $LiNiO_2$ although anomolies in the susceptibility are reported

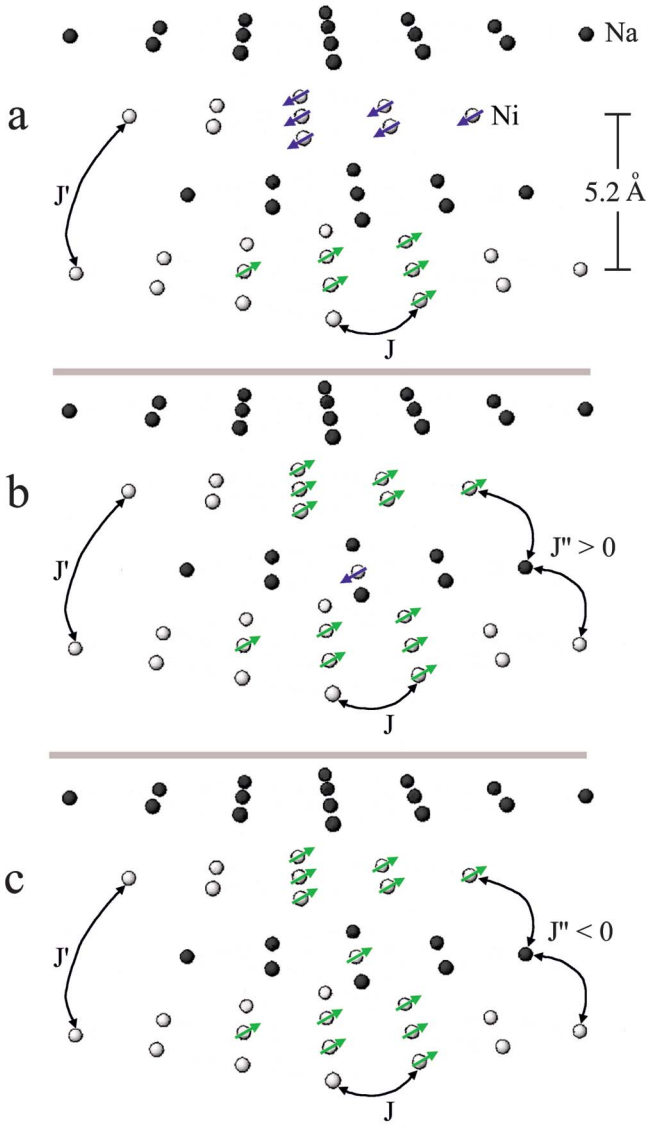

FIG. 1. (Color) (a) The schematic magnetic structure of $NaNiO_2$ below $T_N \sim 23$ K. (b) The stacking sequence frustration induced by impurity Ni spins on the alkali metal sublattice for antiferromagnetic ($J'' > 0$) coupling. (c) The same stacking sequence is favored by ferromagnetic ($J'' < 0$, bottom) coupling.

near 480 K in $LiNiO_2$,[8] which may be related to a *local* structural distortion that cannot attain long-range order due to mixing of the Li and Ni sublattices.

The lack of obvious orbital ordering in $LiNiO_2$ and the orbital degeneracy which would arise in its absence has motivated many theoretical authors to consider coupled orbital and spin degrees of freedom[7–9,18–21] as a mechanism to suppress magnetic ordering at low temperatures. Other recent work suggests orbital and spin degrees of freedom are decoupled.[14]

Stoichiometric amounts of Na_2O_2 and NiO were mixed and pelletized in an Ar atmosphere. These pellets were subsequently annealed at 973 K in O_2 for 70 h with one intermediate grinding. We prepared a 30 g polycrystalline sample of $NaNiO_2$ in this manner and characterized a small part of it with SQUID magnetic susceptibility techniques. The resulting field-cooled (FC) and zero field cooled (ZFC) dc susceptibilities are shown in the top panel of Fig. 2. The magnetic phase transition near $T_N \sim 23$ K is immediately clear as a peak in $\chi(T)$. In addition, a break between the FC and ZFC susceptibilities below ~10 K is seen, indicating some glassiness within the ordered state at these low temperatures.

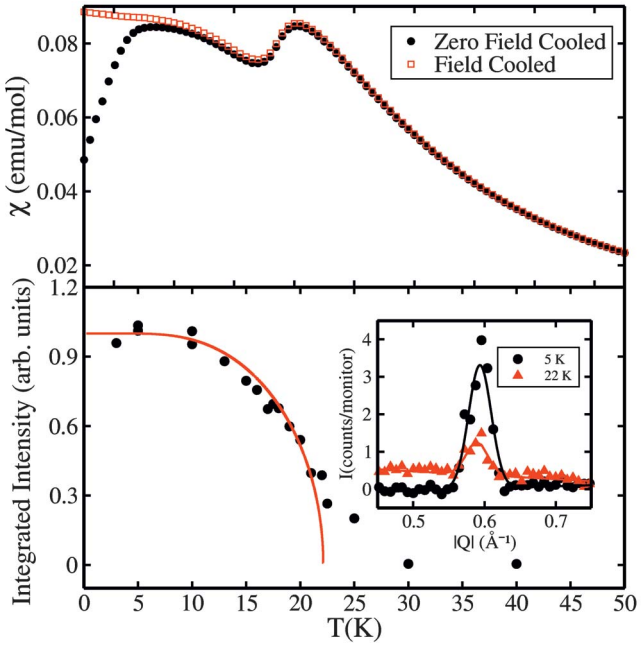

FIG. 2. (Color) Top panel: The field-cooled and zero field cooled susceptibilities of $NaNiO_2$ are shown. Bottom panel: The temperature dependence of the integrated intensity of the (0,0,1/2) magnetic Bragg peak at $Q \sim 0.6$ Å^{-1} is shown, indicating a continuous transition near $T_N \sim 23$ K. The inset shows net scattering at two different temperatures below T_N as described in the text

Time-of-flight neutron scattering measurements were performed on this 30 g sample of $NaNiO_2$ using the Disk Chopper Spectrometer (DCS) at the NIST Center for Neutron Research. The DCS uses choppers to create pulses of monochromatic neutrons whose energy transfers on scattering are determined from their arrival times in the instrument's 913 detectors located at scattering angles from −30° to 140°. Measurements were performed with 3.2 and 5.5 Å incident neutrons. Using 5.5 Å incident neutrons, the energy resolution was 0.075 meV.[22]

III. EXPERIMENTAL RESULTS

Typical data sets at low temperature are shown in Figs. 3(a)–3(c), with the intensity scale chosen to highlight detail in the inelastic scattering. Cuts through the elastic scattering (integrating in $\hbar\omega$ between ±0.1 meV) of this data are shown in the inset to the lower panel of Fig. 2. Here we clearly see the appearace of new Bragg peaks below $T_N \sim 23$ K. These particular data sets correspond to the subtraction of a high-temperature, 30 K, data set from data sets at the indicated low temperatures and are centered around the $Q = 0.6$ Å^{-1} region of reciprocal space, the position at which the lowest-Q Bragg peak appears.

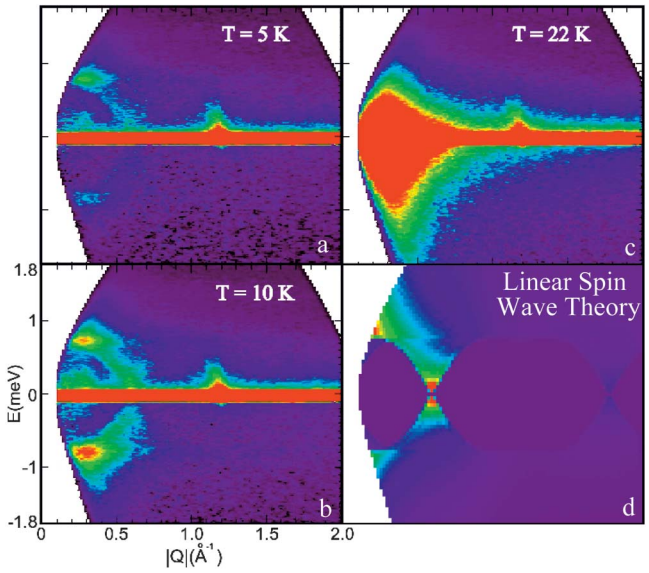

FIG. 3. (Color) The maps of neutron scattering from $NaNiO_2$ at three temperatures near and below $T_N \sim 23$ K, at (a) 5 K, (b) 10 K, and (c) 22 K. The bottom right panel, (d), shows the results of a linear spin wave theory calculation at 10 K, which can be compared directly to the experiments. The linear intensity scale has been chosen to highlight the inelastic spin wave scattering.

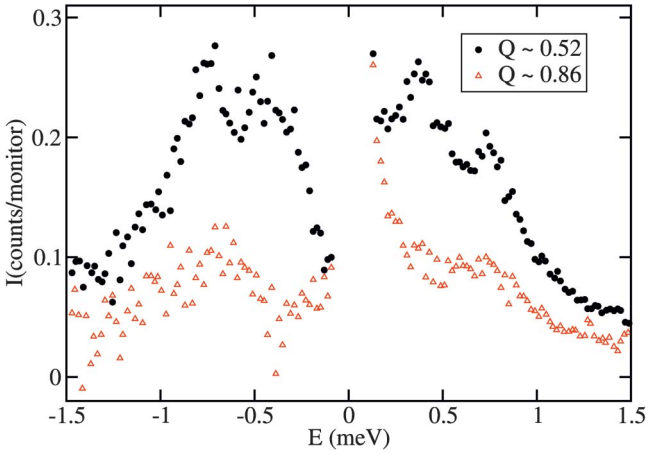

FIG. 4. (Color) The cuts through the maps of scattering at 10 K shown in Fig. 3(b). These data approximate constant-Q scans at $Q=0.52$ and 0.86 Å^{-1} and clearly show a largely dispersionless excitation at $\hbar\omega \sim 0.7$ meV, in addition to the Goldstone mode.

This and several other very weak magnetic Bragg peaks ($\sim 10^{-3}$ of the strongest nuclear Bragg peaks) are evident and can be accounted for both in position and relative intensity by a simple magnetic structure in which the $s=1/2$ moments on the nickel sites are arranged in ferromagnetic sheets within the triangular planes, and the sheets are antiferromagnetically stacked along c, such that moments on neighboring planes are π out of phase with each other. The details of the modeling of this elastic magnetic scattering are consistent with a rather large ordered moment, close to 1 μ_B/Ni, and do not support composite Zhang-Rice singlet magnetic moments associated with NiO.

The Bragg peak shown in the bottom panel of Fig. 2 is indexed as $(0,0,1/2)$ and arises due to a π phase shift across the 5.2 Å between triangular Ni planes, thereby appearing at $Q=\pi/5.2 \sim 0.6$ Å^{-1}. The integrated intensity of this Bragg peak is shown in the bottom panel of Fig. 2. Both this intensity and that of other magnetic Bragg peaks tend to zero near $T_N \sim 23$ K, consistent with a continuous phase transition. The rounded nature of the order parameter near T_N is unusual, and possibily due to dimensional crossover.

The details of the magnetic structure, to be presented elsewhere, are determined by the relative intensities of the measured magnetic Bragg peaks at low temperatures. Here we simply note that the form of the magnetic neutron scattering cross section requires that Bragg intensity at $(0,0,1/2)$ be due to components of ordered moment within the triangular plane, and that the relative intensities require that the moments make a relatively large angle with respect to the triangular plane.

The inelastic scattering in Fig. 3 clearly shows spin wave excitations going to zero energy at the $(0,0,1/2)$ magnetic zone center, and reaching a zone boundary energy of ~ 0.7 meV at $Q \sim 0.3$ Å^{-1}. In addition, rather weak but clearly observable inelastic scattering is seen in a dispersionless inelastic feature at ~ 0.7 meV which extends across all Q measured. This is most clearly seen in cuts through this data, which approximate constant-Q scans, and which are shown for two different Q's in Fig. 4. All of these excitations can be seen on both the neutron energy loss (+ve side) and neutron energy gain (−ve side) of zero energy transfer, as required by detailed balance. The inelastic data in Fig. 3 has been corrected for detector efficiency only.

The inelastic scattering meaurements near T_N show the spin wave band along c^* to soften completely, such that the envelope of the spin wave dispersion fills in with inelastic intensity, as shown in Fig. 3(c). These measurements indicate the nature of the transition at $T_N \sim 23$ K is a loss of registry between well-correlated ferromagnetic triangular planes. This likely also explains the previous observation of small angle neutron scattering in $LiNiO_2$ (Ref. 4) as originating from the collapse of the inelastic spin wave scattering, which occurs below $Q \sim 0.6$ Å^{-1}. Such inelastic scattering would be integrated up in a diffraction, SANS experiment producing a temperature-dependent signal at small Q, whose intensity peaks near T_N.

IV. LINEAR SPIN WAVE THEORY AND COMPARISON TO EXPERIMENT

We have also carried out linear spin wave theory calculations appropriate to $s=1/2$ moments interacting on the Ni^{3+} sublattice of $NaNiO_2$, with the following microscopic Hamiltonian:

$$\mathcal{H} = J \sum_{ab_{nn}} \mathbf{S_i S_j} + K \sum_{ab_{nn}} S_i^z S_j^z + J' \sum_{c_{nn}} \mathbf{S_i S_j}, \qquad (1)$$

where the exchange integral within the triangular ab basal plane is ferromagnetic, and relatively strong, $J=-2.5$ meV, and that along the stacking c direction is antiferromagnetic and relatively weak, $J'=+0.16$ meV. In addition we have

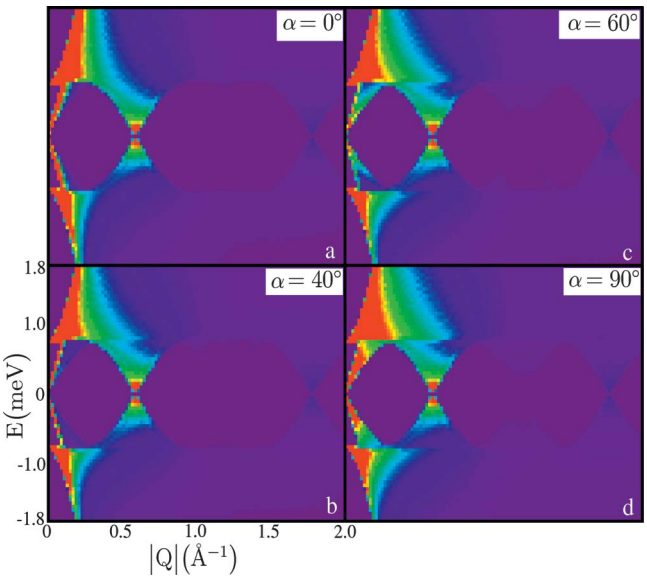

FIG. 5. (Color) The maps of calculated neutron scattering from $NaNiO_2$ using linear spin wave theory are shown at 10 K and for four different easy plane orientations relative to the triangular basal plane. $\alpha=0°$, shown in (a), corresponds to a coincidence between the easy plane and the triangular plane, while $\alpha=90°$, in (d), corresponds to these two planes being normal to each other. The calculation for $\alpha=40°$ in (b) is the same as that shown in Fig. 3(d)). These calculations show that a relatively large angle α is required between the magnetic easy plane and the triangular basal plane, in order for the dispersionless excitation near 0.7 meV to be observable.

included an anisotopy term, K, whose strength is set equal to J', and whose purpose is to preferentially restrict the spins to a plane perpendicular to z. All interactions are nearest neighbor only. The inclusion of this anisotropy term is phenomenological, producing two transverse branches in the spin wave spectrum along c^* as is observed experimentally. Note that the Dzyaloshinski-Moriya interaction, which requires a lack of inversion symmetry between the sites whose coupling it mediates, is not allowed by the space group of $NaNiO_2$. Hence anisotropic exchange is expected to be the leading order anisotropic interaction.

$\mathrm{Im}\chi(\mathbf{Q},\hbar\omega)$ for such a system was calculated within linear spin wave theory at $T=10$ K and this result was angularly averaged to produce theoretical expectations appropriate to an inelastic neutron scattering study carried out on a polycrystalline sample. This is shown in Fig. 3(d) and in all the panels of Fig. 5.

This calculation employs a z-direction in Eq. (1), normal to the easy plane, which defines the easy plane. In general, the resulting magnetic easy plane makes some angle, α, with respect to the triangular basal plane. Therefore the magnetic easy plane is not neccesarily coincident with the triangular plane. The calculation shown in Fig. 3(d) employs an angle of $\alpha=40°$. Figure 5 shows the results of this calculation for the expected powder-averaged inelastic neutron scattering using four different values of α: (a) $\alpha=0°$ (easy plane coincident with triangular plane), (b) $\alpha=40°$, (c) $\alpha=60°$, and (d) $\alpha=90°$ (easy plane normal to the triangular plane).

As can be seen, a nonzero α is required in order for the dispersionless mode at $\sim$0.7 meV to have observable weight. If the magnetic easy plane was coincident with the triangular basal plane, as they are at $\alpha=0°$, fluctuations out of this plane would be along c^*, and not observable along this direction, by virtue of the polarization dependence of the neutron scattering cross section. In this $\alpha=0°$ case, only the Goldstone mode is predicted to be observed.

As can be seen comparing Figs. 3(b) and 3(d), the quantitative agreement between the calculation of the spin wave spectrum and the measurements at 10 K is very good, although some minor discrepancies are evident. The measured spin wave excitations are identified as corresponding to those propagating along the stacking direction. Furthermore, the zone boundary spin wave energy, at $Q=0.3$ Å^{-1}, is given by $\Delta_{ZB}=6S\sqrt{(J'^2+J'K)}$ which reduces to $\Delta_{ZB}=6\sqrt{2}SJ'$ for the case where $J'=K$. Reading $\Delta_{ZB}=0.7$ meV off the data, we get $J'=0.16$ meV. This direct measurement of J' can be combined with the measured $\Theta_{CW}\sim 3.5$ meV obtained from fits to the high temperature susceptibility[6,11] to produce an estimate for the stronger in-plane ferromagnetic exchange. Using $k_B\Theta_{CW}=-[6S(S+1)/9](3(J+J')+K)$ we obtain $J=-2.5$ meV.

V. DISCUSSION AND CONCLUSIONS

Our measurements of the spin structure and dynamics in $NaNiO_2$ directly reveal a rather simple magnetic structure corresponding to an antiferromagnetic stacking of ferromagnetic sheets. Such a structure is very sensitive to frustration of the stacking sequence, and therefore frustration in the ability of the structure to attain true three-dimesional long-range order, due to mixing of the alkali metal and transition metal sublattices. This is precisely the nature of chemical disorder shown to be relevant in $LiNiO_2$ at the 1%–3% level.[3,23]

This scenario is illustrated schematically in Fig. 1. This drawing shows three sets of interacting ferromagnetic layers of Ni moments. Figure 1(a) shows the simple antiferromagnetic stacking of ferromagnetic layers determined from our neutron measurements. Figures 1(b) and 1(c) show the consequences of impurity spins which couple either antiferromagnetically (b) or ferromagnetically (c) to neighboring Ni layers. It is clear that misplaced magnetic Ni ions sitting in the alkali metal triangular planes provide an exchange pathway along the stacking direction which will frustrate the stacking sequence *independent of whether these impurity spins couple ferromagnetically or antiferromagnetically to the moments on Ni triangular planes above and below.* This is due to the fact that *two* such pathways link neighboring Ni triangular planes, thus the sign of this interaction is irrelevant. Furthermore, as these impurity nickel spins are a factor of 2 closer along the stacking direction to spins within the Ni triangular planes than those residing within the Ni triangular planes, the magnitude of this frustrating Ni-impurity Ni-Ni interaction is expected to be relatively strong.

If, as has been argued,[8,14] orbital degeneracy is not responsible for it, a natural and simple explanation for the spin glass phase in $LiNiO_2$ ensues as a consequence of this structure. Samples of $LiNiO_2$ display weak mixing between the

Ni and Li sublattices, providing a sample-dependent tuning of the strength of the stacking sequence disorder. This leads to a glass transition which depends on the precise level of disorder in the sample and which will occur at temperatures on the order of that associated with phase coherence between strongly correlated ferromagnetic layers, $T_N \sim 23$ K. This scenario is qualitatively similar to the ferrimagnetic clusters previously proposed[23,24] to explain the spin glass phase in $LiNiO_2$, with the exception that the stacking sequence frustration occurs independent of the sign of the coupling between impurity spins and the magnetic layers.

To conclude, new elastic and inelastic neutron scattering measurements have directly determined the simple antiferromagnetic structure of $NaNiO_2$ below $T_N \sim 23$ K. These measurements allow a microscopic understanding of the magnetically ordered state in $NaNiO_2$ and may provide the basis for a simple explanation of the phase behavior exhibited in $LiNiO_2$.

ACKNOWLEDGMENTS

We wish to acknowledge useful contributions from I. Crooks, J. van Duijn, S-H. Lee, S. Park, and G. Sawatzky. This work was supported by NSERC of Canada, and utilized facilities supported in part by the NSF under Agreement Nos. DMR-9986442 and DMR-0086210.

[1] See, for example *Dynamical Properties of Unconventional Magnetic Systems*, edited by A. T. Skjeltorp and D. Sherrington, NATO ASI Series, Series E, Applied Sciences Vol. 349 (Kluwer Academic Publishers, Boston, 1998).
[2] K. Hirakawa, H. Kadowaki, and K. Ubukoshi, J. Phys. Soc. Jpn. **54**, 3526 (1985).
[3] J. N. Reimers, J. R. Dahn, J. E. Greedan, C. V. Stager, G. Lui, I. Davidson, and U. von Sacken, J. Solid State Chem. **102**, 542 (1993).
[4] H. Yoshizawa, H. Mori, K. Hirota, and M. Ishikawa, J. Phys. Soc. Jpn. **59**, 2631 (1990).
[5] K. Hirota, Y. Nakazawa, and M. Ishikawa, J. Phys.: Condens. Matter **3**, 4721 (1991).
[6] J. P. Kemp, P. A. Cox, and J. W. Hodby, J. Phys.: Condens. Matter **2**, 6699 (1990).
[7] Y. Kitaoka, T. Kobayashi, A. Koda, H. Wakabayashi, Y. Niino, H. Yamakage, S. Taguchi, K. Amaya, K. Yamaura, M. Takano, A. Hirano, and R. Kanno, J. Phys. Soc. Jpn. **67**, 3703 (1998).
[8] F. Reynaud, D. Mertz, F. Celestini, J. M. Debierre, A. M. Ghorayeb, P. Simon, A. Stepanov, J. Voiron, and C. Delmas, Phys. Rev. Lett. **86**, 3638 (2001).
[9] M. V. Mostovoy and D. I. Khomskii, Phys. Rev. Lett. **89**, 227203 (2002).
[10] E. Chappel, M. D. Nunez-Regueiro, G. Chouteau, O. Isnard, and C. Darie, Eur. Phys. J. B **17**, 615 (2000).
[11] E. Chappel, M. D. Nunez-Regueiro, F. Dupont, G. Chouteau, C. Darie, and A. Sulpice, Eur. Phys. J. B **17**, 609 (2000).
[12] M. A. van Veenendaal and G. A. Sawatzky, Phys. Rev. B **50**, 11326 (1994).
[13] T. Mizokawa, H. Namatame, A. Fujimori, K. Akeyama, H. Kondoh, H. Kuroda, and N. Kosugi, Phys. Rev. Lett. **67**, 1638 (1991); T. Mizokawa, A. Fujimori, H. Namatame, K. Akeyama, and N. Kosugi, Phys. Rev. B **49**, 7193 (1994).
[14] M. Holzapfel, S. de Brion, C. Darie, P. Bordet, G. Chouteau, P. Strobel, A. Sulpice, and M. D. Nunez-Regueiro, cond-mat/0403329.
[15] P. W. Anderson, Mater. Res. Bull. **8**, 153 (1973).
[16] See, for example, *Magnetic Systems with Competing Interactions*, edited by H. T. Diep (World Scientific, Singapore, 1994).
[17] S. Dick, M. Muller, F. Preissinger, and T. Zeiske, Powder Diffr. **12**, 239 (1997).
[18] L. F. Feiner, A. M. Oles, and J. Zaanen, Phys. Rev. Lett. **78**, 2799 (1997); A. M. Oles, L. F. Feiner, and J. Zaanen, Phys. Rev. B **61**, 6257 (2000).
[19] Y. Q. Li, M. Ma, D. N. Shi, and F. C. Zhang, Phys. Rev. Lett. **81**, 3527 (1998).
[20] M. van den Bossche, P. Azaria, P. Lecheminant, and F. Mila, Phys. Rev. Lett. **86**, 4124 (2001).
[21] F. Vernay, K. Penc, P. Fazekas, and F. Mila, Phys. Rev. B **70**, 014428 (2004).
[22] J. R. D. Copley and J. C. Cook, Chem. Phys. **292**, 477 (2003).
[23] M. D. Nunez-Regueiro, E. Chappel, G. Chouteau, and C. Delmas, Eur. Phys. J. B **16**, 37 (2000).
[24] E. Chappel, M. D. Nunez-Regueiro, S. deBrion, G. Chouteau, V. Bianchi, D. Caurant, and N. Baffier, Phys. Rev. B **66**, 132412 (2002).